ACS SyntheticBiology

pubs.acs.org/synthbio Research Article

A Genetic Programming Approach to Engineering MRI Reporter Genes

Published as part of the ACS Synthetic Biology virtual special issue "AI for Synthetic Biology".

Alexander R. Bricco, Iliya Miralavy, Shaowei Bo, Or Perlman, David E. Korenchan, Christian T. Farrar, Michael T. McMahon, Wolfgang Banzhaf,* and Assaf A. Gilad*

Cite This: *ACS Synth. Biol.* 2023, 12, 1154–1163 Read Online

ACCESS | Metrics & More | Article Recommendations | Supporting Information

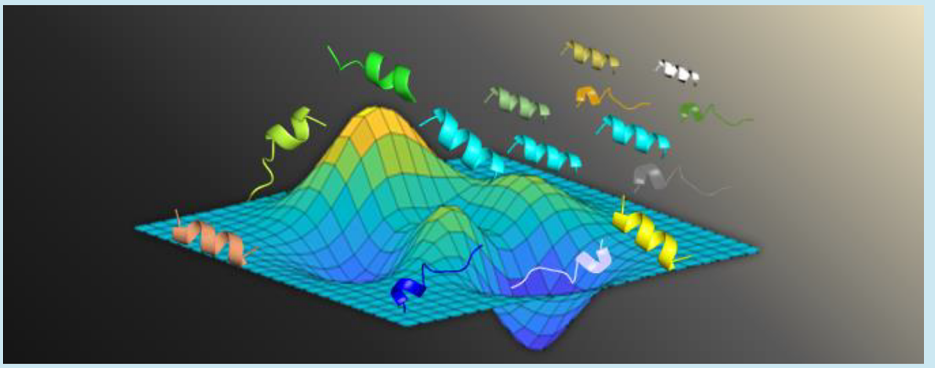

ABSTRACT: Here we develop a mechanism of protein optimization using a computational approach known as "genetic programming". We developed an algorithm called Protein Optimization Engineering Tool (POET). Starting from a small library of literature values, the use of this tool allowed us to develop proteins that produce four times more MRI contrast than what was previously state-of-the-art. Interestingly, many of the peptides produced using POET were dramatically different with respect to their sequence and chemical environment than existing CEST producing peptides, and challenge prior understandings of how those peptides function. While existing algorithms for protein engineering rely on divergent evolution, POET relies on convergent evolution and consequently allows discovery of peptides with completely different sequences that perform the same function with as good or even better efficiency. Thus, this novel approach can be expanded beyond developing imaging agents and can be used widely in protein engineering.

KEYWORDS: *protein engineering, CEST MRI, genetic programming*

INTRODUCTION

Natural evolution has produced a myriad of proteins, and many of them have been used for medical treatment and recently for diagnostics. However, since the beginning of life, natural evolution has only explored a small portion of the protein design space,[1] challenging protein engineers to optimize existing and to even create new protein functions. Directed evolution is a common and powerful technique to artificially evolve proteins in the laboratory.[2] In general, directed evolution starts from a template protein that has a function similar to the desired one. Next, a library of mutant proteins is generated, often by using error-prone DNA polymerase, and screened for the "fittest" protein that shows the most desired feature. This first generation will then serve as a template for the next generation, and the procedure is repeated until a suitable protein with respect to the particular feature is found (Figure 1a).

Despite its effectiveness, directed evolution comes with several limitations. For many proteins, the experimental evaluation process is very time-consuming and many of the mutants produce silent mutations which do not carry on to later generations. Furthermore, optimizing proteins requires navigation through a complex fitness landscape, with optimization trajectories often leading to a dead-end, unless several mutations occur at once[3,4] (Figure 1b). Deploying a novel *Protein Optimization Engineering Tool (POET)* based on genetic programming can make it possible to overcome these

Received: December 1, 2022
Published: March 22, 2023

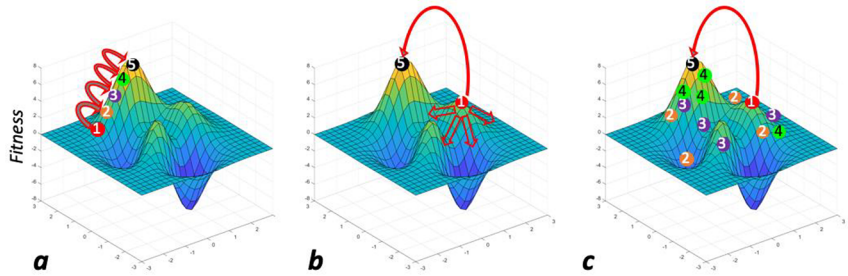

Figure 1. The principles of POET. (a) Illustration of conventional directed evolution, where in each evolution cycle one mutant exhibits better fitness and thus is used as a template for the following generation of evolution. (b) Often, in directed evolution, the protein fitness reaches a local maximum, and consequently all the mutants exhibit lower fitness (empty arrows). In this case it is impossible to predict which mutant should be used as a template to achieve improved fitness (the route from 1 to 5). (c) In the case of POET, the route from 1 to 5 is not determined by stepwise mutagenesis and adhering to the parental protein, but rather by generating libraries of peptides that cover broadly all the search space. Each generation helps to shape a set of rules that determine the next set of peptides. This way all the search space of the fitness landscape is covered and consequently minimizing the probability of missing the absolute maximum.

challenges by exploring a wider range of the protein design space (Figure 1c). POET relies on the principle of convergent evolution, i.e., when species/proteins have different origins but have developed similar features. This is in contrast to divergent evolution, in which separate species evolve differently from a common origin. Thus, POET allows for the identification of new peptides/proteins with desired features that could not have been discovered with traditional protein engineering tools. POET utilizes all the search space, and even protein variants that do not show improvement over previous generations to provide useful information that can lead to improvement of the next generation. Hence, the POET algorithm is potentially a game changer for the protein design tool that can be implemented into numerous protein engineering applications.

Evolutionary Computation is a field in computer science, studying algorithms inspired by biological evolution. *Genetic Programming* (GP)[5,6] is among powerful evolutionary computation techniques that evolve solutions to difficult structural design tasks as a general problem solver. In the context of protein engineering, GP was used to predict transmembrane domains and omega loops in proteins,[5] to evolve energy functions for evaluating protein structures,[7] and more recently, to predict protein−protein interactions related to disease.[8] This earlier work demonstrates the capability of GP to model features in the protein search domain, and in particular its ability to extract features relevant for a prediction task. This is a central capability in biological applications where often high-dimensional inhomogeneous data sets are used as input to predict output values. In addition to creating predictive models, the underlying mechanisms of GP allow it to come up with novel models, often on first sight surprising or even counterintuitive to the user.[9] Over the past decades, GP has proven to produce human-competitive solutions to many problems.[10]

To evaluate the potential of POET to evolve ultrasensitive proteins and peptides, we decided to focus on solving the problem of sensitivity of a specific class of peptide-based probes used for magnetic resonance imaging (MRI) of molecular targets. The peptides can be detected with MRI via a contrast mechanism, termed chemical exchange saturation transfer (CEST). CEST is based on the dynamic exchange process between an exchangeable proton (hydrogen atom) and the surrounding water protons.[11,12] This contrast was demonstrated to be most efficient for poly-L-lysine by van Zijl and colleagues[13] and later on was optimized for several other peptides.[14,15] The poly-L-lysine was used as a backbone for designing of a synthetic gene, termed Lysine Rich Protein (LRP), that was successfully used for *in vivo* imaging of several translational models.[16−20] However, long repeats and high content of lysine residues might affect the cellular stability of the protein and consequently reduce the contrast. To increase the number of available building blocks and improve the contrast, we developed POET to evolve peptides that provide high CEST contrast with diverse sequences.

RESULTS AND DISCUSSION

Developing Protein Optimization Evolving Tool (POET) Based on Genetic Programming. Genetic programming, much like many other evolutionary algorithms, follows the basic principles of evolution. A population of random solutions to a given problem is generated as the first generation. The fitness of each of these solutions is evaluated and quantified as a measurement for their performance. The solutions with the highest fitness values are more likely to be selected to create the next generation of solutions after being impacted by evolutionary operators such as crossovers and mutations. Crossover is a reproduction mechanism analogous to sexual reproduction. Usually in crossover two parent solutions are selected to create two new offsprings. A common way to do so is to combine genetic codes for each of the parent solutions in a manner that the offspring will contain parts from both parents but is not identical with either of them. Mutation usually occurs after crossover and has a chance to randomly modify a small detail of solutions. The general goal of GP is to evolve solutions to reach a specified fitness level. In other words, to find a solution that satisfies the solving criteria of a problem.

As a first step of developing POET, we incorporated GP to evolve CEST predicting models represented by tables of motifs and weights. Motifs are recurring patterns in protein sequences and their respective weight represents the impact of that pattern in calculating the CEST contrast of a given protein. For example, a motif could be Glycine-Arginine-Arginine (GRR) or Arginine-Lysine (RK) and their initial weights could be −0.60 and 4.39 units, respectively (Figure 2a,b and Table S1). POET models attempt to find their motifs in given protein sequences and add the weights of the found motifs to generate a score value correlated with the CEST contrast of that protein. POET attempts to find and evolve models that best predict the

https://doi.org/10.1021/acssynbio.2c00648
ACS Synth. Biol. 2023, 12, 1154−1163

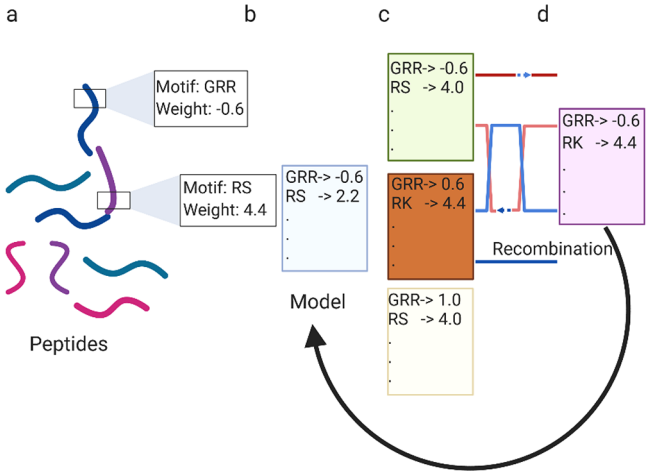

Figure 2. Schematic illustration of POET. (a–d) Paradigm and workflow.

CEST contrast. POET generates an initial random population of 100 models which can have up to 50 rows of motifs and weights. Evaluation of these models is done by comparing the score values from these models with the actual CEST contrast levels of proteins in a training data set. These models are then compared by how well they can predict the CEST contrast measured from the training data (Figure 2c).

POET uses a selection mechanism called the *Tournament Selection* to choose the parent models from the population (Figure 2c,d). Five models are selected, and their fitness values are compared against each other. The two models with the highest fitness are selected to reproduce two offspring models. POET divides the table of each parent model into two sections of A and B and then generates two offspring models, each of which will contain section A of one parent table and section B of the other. POET uses mutational operators that modify the weights and motifs of the model tables. Across 5,000 to 50,000 iterations of this algorithm (Figure 2, arrow), the motif-weight pairs that are most important and accurate at predicting the training data set are maintained, and those that are poor at improving the training data set are discarded, causing the model to develop in an analogous manner to Darwinian evolution.[21]

POET Develops a Library of Contrast Producing Peptides. Much like in evolution, the fittest peptide can be either selected from a large population (in this case training set) or, alternatively, many generations can compensate for a smaller population. The evolution using POET was performed for ten generations, and the resulting contrast relative to K12 (a sequence of 12 lysines) can be seen in Figure 3. K12 was chosen as a peptide for comparison due to the high contrast it produces and similarities to other reported results from poly-L-lysine.[13,15,17] For each generation we have obtained a library of ten synthetic peptides which were termed for convenience "*CESTides*". Figure 3a,b show z-spectra (CEST-spectra) and MTR_{asym} plots, respectively. The amplitude of the peak of the plot at 3.6 ppm − the amide resonance frequency was used to generate the generational plot Figure 3. As can be seen in Figure 3, within 10 generations, POET generated a CESTide that displays a 4-fold increase in the MRI contrast. Interestingly, the best CESTide was produced in generation 7.

Sequence Diversity of CESTides. POET was able to generate a large variety of different chemistries (Figure S1), many of which would not be discovered by directed evolution on a feasible time scale. Traditionally, the general convention is that peptides that are suitable for generating CEST contrast should be positively charged.[22,23] However, our findings (Figure 4 and Figure S2) demonstrate that good CESTides can deviate from the poly-L-lysine like sequence. This is especially important for designing a new version of genetically encoded CEST based reporters.[20] Less charged reporters reduce intracellular interactions with other proteins while the use of more varied amino acids increases the intracellular expression level of the reporter as it is not dependent on the supply of a single amino acid. Moreover, the diversity in the CESTides isoelectric point (pI) can allow tailoring the reporter to different cellular environments.

Exchange Rate Calculations. There are three factors that determine the optimal CEST contrast (MTR_{asym}): the chemical shift of the exchangeable proton ($\Delta\omega$), the saturation power (ω_1), and the optimal exchange rate (k_{ex}). While simulations can predict what the optimal three factors are, only $\Delta\omega$ and ω_1 are easy to control experimentally. In contrast, the exchange rate is completely dependent on the chemical formulation of the contrast agent.[24] Hence, it is complicated to predict *in silico* the k_{ex} for a contrast agent with a single exchangeable proton[25,26] and even harder to do so for a peptide with at least ten exchangeable protons.[27] We used computational simulations to examine what the optimal exchange rate would be. Our simulations show that for peptides with exchangeable amide protons at 3.6 ppm, the k_{ex} that provides the maximal MTR_{asym} should be around 1473 Hz. Therefore, we aimed with POET to evolve peptides with k_{ex} as close as possible to these values. Since k_{ex} is an absolute

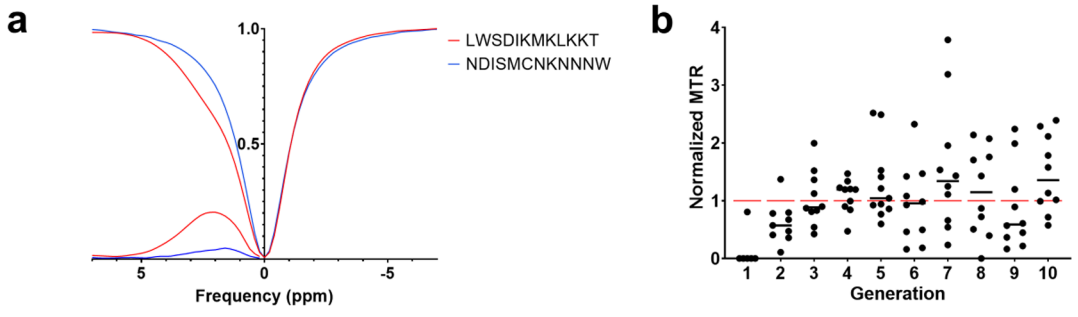

Figure 3. Improvement of CESTides by POET. (a) MTR and z-spectra from the best and the worst peptide in generation 7. (b) The MTR_{asym} is normalized against the contrast generated by K12 in the same experiment to provide a consistent comparison across experiments and plotted with respect to the generations.

https://doi.org/10.1021/acssynbio.2c00648
ACS Synth. Biol. 2023, 12, 1154−1163

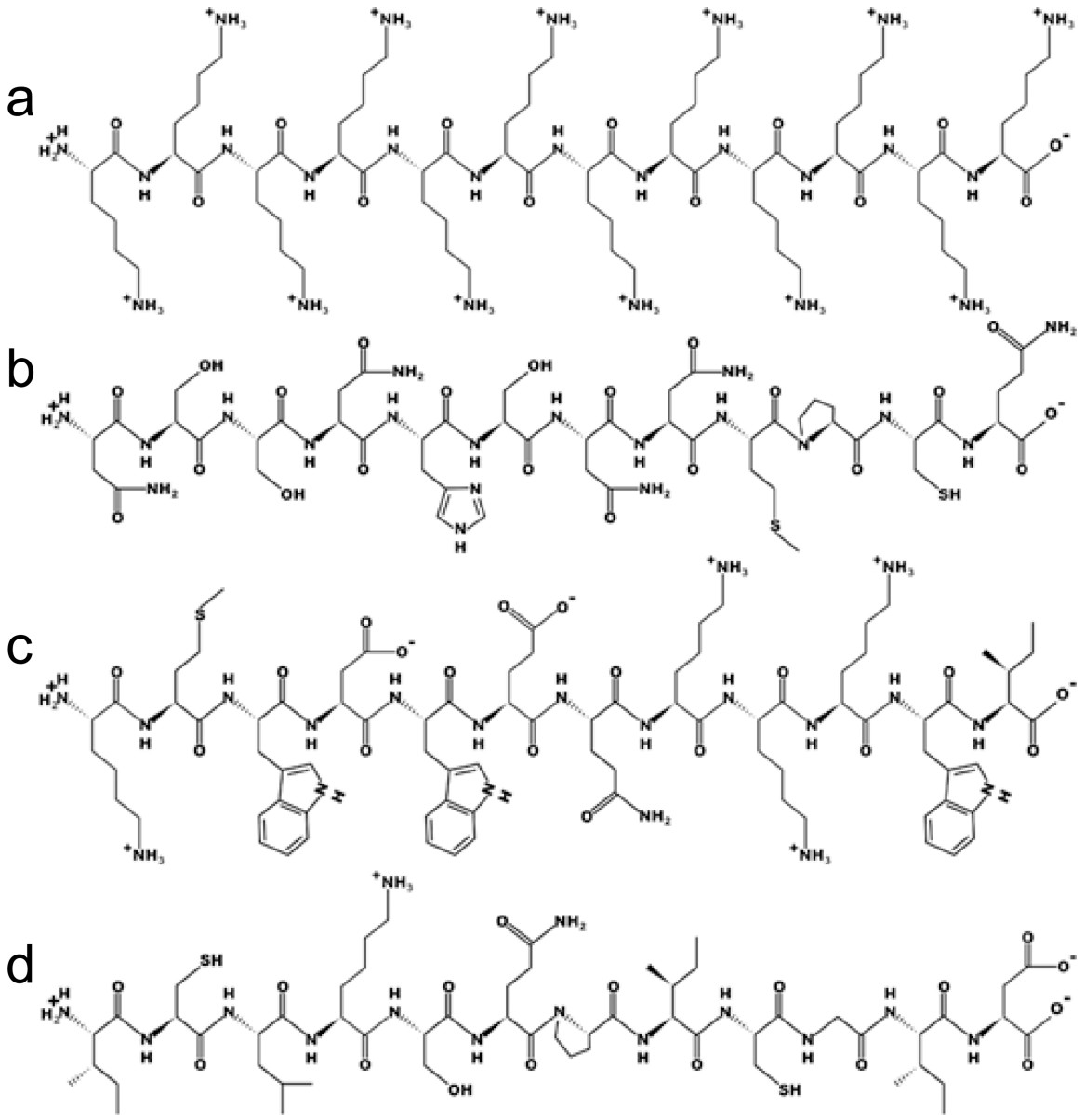

Figure 4. Structure of four representative distinct peptides. (a) K12; KKKKKKKKKKKK; Theoretical pI/Mw: 11.04/1556.10. (b) A peptide from generation 2 has a neutral pI, yet generates contrast higher than the K12; NSSNHSNNMPCQ; Theoretical pI/Mw: 6.73/1332.38. (c) A peptide from generation 5 that generates contrast that is approximately 4 times larger than K12: KMWDWEQKKKWI; Theoretical pI/Mw: 9.53/1706.04. (d) A peptide from generation 7 that generates contrast that is twice that of K12 but has an acidic pI: ICLKSQPICGID.

number that is dependent only on the peptide sequence and structure as well as on the chemical environment of the peptide (i.e., pH, temperature, etc.) and is independent of the field strength, we determined the k_{ex} for selected peptides using a 14.1 T MR spectrometer, which provides better spectral resolution. Table 1 shows improvement in the exchange rate of peptides with evolution. The measured exchange rates are of course an average of the exchange rates of all the exchangeable protons with the same chemical shift. Remarkably, two peptides, KYTKTRKQSSKA and NSSNHSNNMPCQ showed average k_{ex} that are 1.75 times faster than K12. Therefore, using POET we were able to optimize the proton exchange rate of selected peptides through evolution and consequently improve the CEST contrast.

Improvement of Sensitivity. After determining the increased exchange rate of the peptides we developed with POET, we wanted to see if the increase in exchange rate and contrast was able to allow us to detect CEST contrast from lower concentrations of the peptides. We imaged serial dilutions of K12 and compared it to NSSNHSNNMPCQ which is a neutrally charged peptide with an amine proton exchange rate that is approximately 2 fold higher than K12 (913 Hz and 490 respectively). For each dilution we calculated the p value of each pixel using a Student's t test, compared a set of four images obtained +3.6 ppm to four images obtained at −3.6 ppm from the water peak, and created a t test map as described before.[28,29] As can be seen in Figure 5, both peptides can be imaged at concentration as low as 1 mg/mL (505 μM for K12, 668 μM for NSSNHSNNMPCQ) with a confidence level greater than 0.05. It is important to note that the signal-to-noise ratio (SNR) was found to be 59.2 and the CNR was found to average 1.23 in wells with the peptides, compared to 0.39 in wells without peptides. (Figure S3). These data suggest that even at low concentrations, the peptides evolved by POET

https://doi.org/10.1021/acssynbio.2c00648
ACS Synth. Biol. 2023, 12, 1154−1163

Table 1. Normalized CEST Contrast and Exchange Rate for Selected Peptides

		normalized CEST contrast (%)[a]			k_{ex} (Hz)
peptide sequence	generation	amide	amine	OH	amide
KKKKKKKKKKKK[b]	0	3.14	0.00	0.00	490
NSSNHSNNMPCQ	2	6.55	1.46	1.30	856.3
CCWHNPKWRRTR	3	1.34	6.38	11.67	332.6
KYTKTRKQSSKA	3	7.19	3.53	5.89	857.7
KPWHGCASRTKR	4	5.08	5.90	8.75	659.2
DKVCKIQKRKWH	5	4.58	2.75	4.61	572.8
KKRLHWIRWHCG	5	2.52	6.25	6.50	460.1
ICLKSQPICGID	7	1.57	0.62	2.18	704.1
KMGKLIGIPVLK	7	1.55	0.18	0.91	553.2
LWSDIKMKLKKT	7	2.00	0.40	0.95	630.3
EPSNLPKGMNEK	8	2.52	0.35	1.12	529.4
TSKSKKRMTAKK	8	4.52	1.73	3.16	625.8

[a]Normalized to 1 mM peptide concentration, B_1 = 6 μTesla. [b]K12.

produce MTR_{asym} detectable contrast at micromolar concentration.

Learning by POET. We sought to examine the differences between the peptides generated by POET to determine if POET was converging toward a solution. This was calculated via the nearest neighbor distance from peptides in the same generation using Grantham distance, which takes into consideration differences between the size, charge, and hydrophobicity of different amino acids.[30] The basic assumption is that amino acids that are similar in chemical composition, polarity, and molecular volume are more likely to change throughout evolution as they are less disruptive to protein function. To determine whether POET was learning and converging on a solution, we compared the Grantham distance between the peptides discovered with POET with peptides that were generated randomly. We first examined the intergenerational nearest neighbor distance (Figure 6a), by comparing finding the shortest Grantham distance within each peptide's generation and all prior generations. As the Grantham distance decreased with an increase in the number

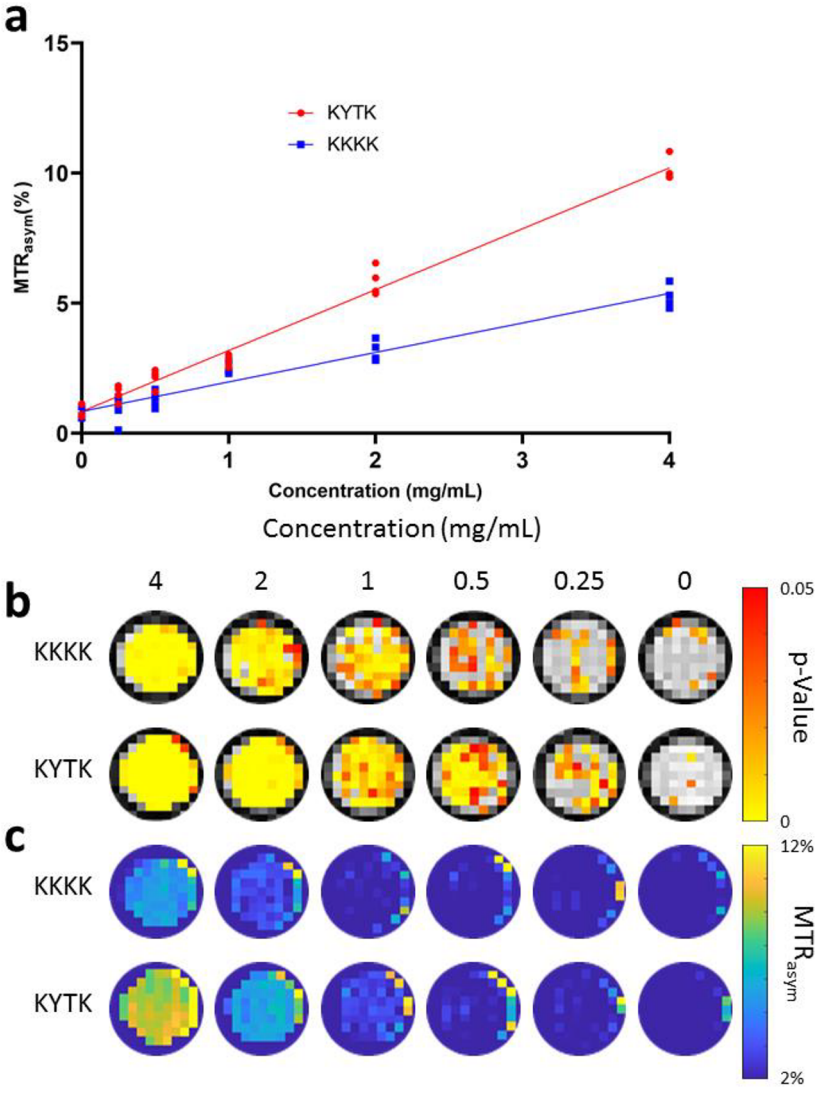

Figure 5. Sensitivity of evolved CEST peptides. (a) Contrast for each sample from the dilution experiment. Lines are from linear regressions, and each has an R^2 greater than 0.95. (b) Probability maps show the p-values from a t test to determine if any contrast perceived is statistically significant. (c) CEST maps show the MTR_{asym} values for each pixel.

https://doi.org/10.1021/acssynbio.2c00648
ACS Synth. Biol. 2023, 12, 1154−1163

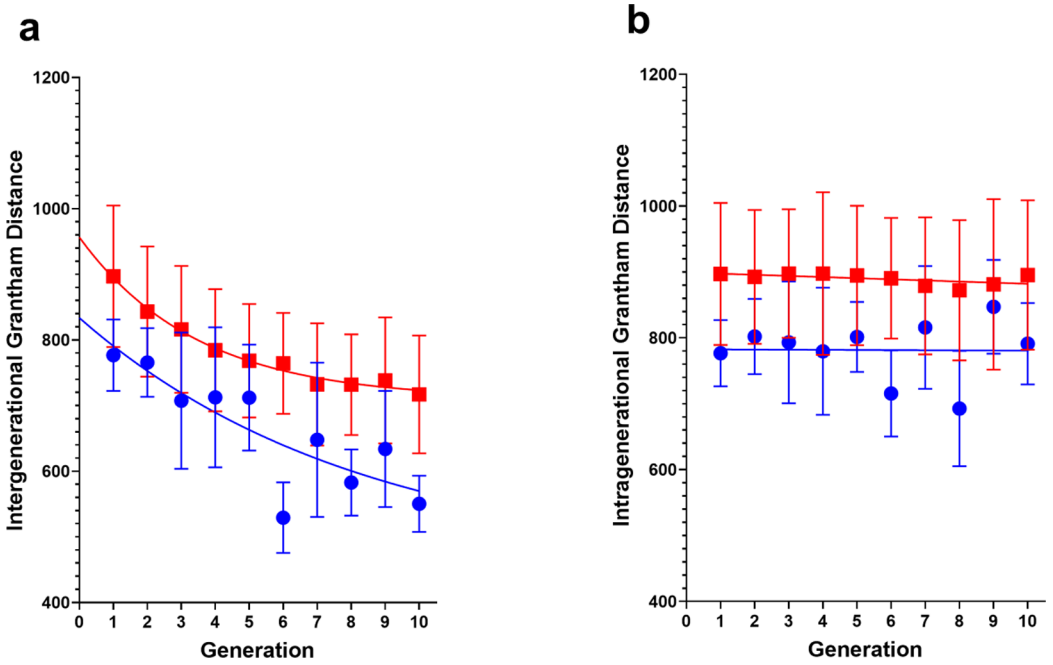

Figure 6. Grantham distance between discovered CESTides. (a) Intergenerational distance, where peptides are compared to those in their own generation and all prior ones. (b) Intragenerational distance, where peptides are only compared to those in the same generation. The peptides discovered using POET are blue circles (mean ± 95% confidence interval (CI)), simulated peptides generated randomly are shown as red squares (mean ± 95% CI). Each data set has a trendline fit to an exponential decay curve (a), or linearly (b).

of generations, this implies that learning took place since it shows that the predictions of POET are more similar than would be generated by randomness and are decreasing in distance faster. Next, we examined the intragenerational nearest neighbor distance by comparing each peptide to all peptides in the same generation to determine the most similar peptide (Figure 6b). We find that the distance stays lower than the random simulation, implying that there is a form of selection occurring since the distance is lower than that of random peptides. The distance is not decreasing by generation which suggests that POET is not converging on a solution, which would show the predictions decreasing in distance as they all approach the same global maximum.

In recent years, CEST has been used for measuring *in vivo* temperature changes,[31] pH,[32,33] enzyme activity,[34,35] metal ions,[36] metabolites,[37] glycogen and glucose,[38,39] glutamate, glycoproteins,[40] and glycosaminoglycan.[41] Recently, CEST MRI has been performed in the beating heart to detect fibrosis after myocardial infarction in mice[42] and for *in vivo* mapping of creatine kinase metabolism.[43] We have previously demonstrated that CEST can be used to monitor sustained drug release[44] and to sense cellular signaling using a genetically encoded biosensor.[45] Moreover, we have repeatedly demonstrated that reporter genes based on CEST MRI can be used to monitor gene expression in a 3D cell culture,[23,46] *in vivo* in rodents,[26] or in a live pig heart.[47] In many of these examples, the CEST contrast is generated from a unique exchangeable proton. In this case, to improve the CEST contrast it is sufficient to optimize the exchange rate of this unique proton and this could be done using rational design.[23] However, when designing a peptide for imaging, with multiple protons that exchange with different resonance frequencies and different rates, the optimization is too complex and is beyond the current rational design capabilities. Thus, using tools like POET that combine machine learning algorithms and evolutionary principles with experimental measurement, is ideal for peptide optimization.

We do note that some of the POET optimized peptides (e.g., KKRLHWIRWHCG) have lower amide exchange rates relative to K12. However, the amine contrast at 2 ppm was significantly greater for these peptides indicating that the increased MTR_{asym} at 3.6 ppm for these optimized peptides has contributions also from the amine exchangeable protons. This can be seen in Figure 3b where a strong amine MTR_{asym} is observed at 2 ppm for some of the optimized peptides. Thus, POET can optimize and exploit both amide and amine exchangeable protons to maximize the MTR_{asym} at 3.6 ppm.

In one of the original papers, van Zijl and colleagues suggested poly-L-lysine as polypeptide based CEST agents.[13] Following this discovery, we explored multiple genetically encoded proteins rich in positively charged amino acids such as lysine and arginine.[16,18−20,48,49] Many of these genes expressed proteins *in vivo*. In none of these studies was a toxic effect or immune response observed. Nevertheless, in many of these studies there was no long-term follow up on immune response. While direct injection of high doses of poly-L-lysine may be toxic,[50] other studies suggest that a toxic or immunogenic response depended on the formulations; for example, poly-L-lysine nanocapsules show immunocompatibility and lack of toxicity *in vivo*.[51] One of the goals of this study was to explore the boundaries of amino acid composition without compromising the CEST contrast. It is well understood and characterized that the presence of foreign proteins in the body will eventually elicit an immune response. Nevertheless, the findings from this study strongly support the notion that immunogenetic epitopes could be replaced with other peptides while retaining CEST characteristics. In fact, it might be feasible to expand the POET to include a module that screens for immunogenic epitopes using known algorithms and exclude these epitopes much like we excluded hydrophobic peptides to

https://doi.org/10.1021/acssynbio.2c00648
ACS Synth. Biol. 2023, 12, 1154−1163

humanize future CEST reporters. Moreover, POET helps to diversify the amino acid sequence, finding sequences that are uncharged as described above and potentially replace immunogenic epitopes with nonimmunogenic epitopes.

One of POET's advantages is the ability to develop peptides where the mechanism of the peptide is not understood. Currently, one of the limiting factors is the length of the peptide. Every additional amino acid increases exponentially the peptide search space. This, in turn, increases the time required for computing each generation. With the increase in computational power, it is anticipated that POET can be applied for longer peptides. Sometimes it is important to have AI for evolving large proteins, but sometimes it is important just to evolve short peptides or motifs in large protein sequences. POET can be useful for optimizing short peptides and especially when only small data sets are available by reliance more on generational evolution. Such examples for short peptides or motifs could be peptides for drug, gene, or exosome targeting,[52] metal binding domains,[53] functional protein motifs,[54] or peptide linkers for fusion proteins.[55,56] All the above applications rely on short peptides and could benefit from optimization by POET.

MATERIALS AND METHODS

Peptide Synthesis and Preparation. The peptides determined by POET were obtained from Genscript (Piscataway, NJ). Each peptide was dissolved to a concentration of 5 mg/mL in deionized water. Mass concentrations were used for experiments due to limitation of volume in the phantom and the small amount of soluble peptide. Calculations of molar mass assumed each peptide would associate with a Na^+ ion on every negatively charged residue and a Cl^- ion on every positively charged residue. To keep differences in pH from interfering with the CEST effect, each peptide was titrated to a pH of 7.2 using 0.1 M HCl and 0.1 M NaOH.

MRI Parameters. In earlier generations MRI data was obtained using a vertical bore 11.7 T Bruker Avance system with the 0.2 mL samples placed in the imaging coil and kept at 37 °C during imaging. The first scan is a WASSR scan used to determine the exact frequency of water in the sample so that it may be adjusted accordingly.[57] The second scan is a CEST scan made from a modified RARE sequence (TR/effective TE = 10000/4.5 ms, RARE factor = 32, FOV = 17 × 17 mm^2, slice thickness = 1.2 mm, matrix size = 64 × 64, spatial resolution = 0.27 × 0.27 mm^2) including a continuous-wave saturation pulse of 4 s, saturation powers of 1.2, 2.4, 3.6, 4.7, 6.0, 7.2, 10.8, and 12.0 μT covering saturation frequencies from −10 to +10 ppm offset from water in steps of 0.27 ppm. Starting with the fifth generation of peptides we acquired MRI data using a horizontal bore 7T Bruker preclinical MRI. The change in field strength produced similar results, but at lower field strength there is a higher influence on the amide contrast effect from the amine contrast as the peaks broaden.

The samples were placed within an imaging phantom custom designed and produced by 3D printing specifically for this task. Each group of samples is run through two scans. The first scan is a WASSR scan used to determine the exact frequency of water in the sample so that it may be adjusted accordingly.[57] The second scan is a CEST scan made from a modified RARE sequence, with a RARE factor of 16, and a TR of 10,000 ms. Saturation pulses were applied as a block pulse for 4000 ms, and a saturation power of 4.7 μT covering saturation frequencies from −7 to 7 ppm offset from water in steps of 0.2 ppm. Each generation was scanned multiple times to ensure accuracy. Data processing was done with an in-house MATLAB script.[58]

Finally, the amide proton chemical exchange rate was measured by Quantitation of Exchange with Saturation Power (QUESP)[27] using an ultrafast Z-spectroscopy method[59] on a 14.1 T Bruker NMR spectrometer where the saturation power was varied from 0.2 to 14.8 μT. The saturation time was 5 s, the TR was 10 s, the number of averages was 8, and the temperature was maintained at 37 °C.

Exchange Rate Calculation and Simulation. The amide proton exchange rate was quantified by Bloch−McConnell equation fitting of the power dependence of the 14.1 T amide proton signal using custom written software (MATLAB). The amide proton signal was extracted from the ultrafast Z-spectrum by 4-pool (water, amide, amine, and hydroxyl proton pools) Lorentzian fitting.[60]

To investigate the relationship between the amide proton exchange rate and the asymmetric magnetization transfer ratio MTR_{asym} at different saturation pulse powers, a simulation study was performed based on the numerical solution of the Bloch−McConnell equations implemented in MATLAB (MathWorks).[61] The parameters used were longitudinal water relaxation (T_1) of 1600 ms for both the water and solute pools, transverse relaxation time (T_2) of 50 and 1 ms for the water and solute pools, respectively, and a solute concentration of 200 mM with a chemical shift of 3.6 ppm. The simulated acquisition protocol used an echo time (TE) of 20 ms, a repetition time (TR) of 15 s, a continuous saturation pulse of 5 s, applied at 9 to −9 ppm frequency offsets, with 0.25 ppm intervals, and a readout flip angle of 90°, under a 7T main magnetic field (B_0). The examined exchange rates varied uniformly between 100 to 2000 Hz with 1 Hz increments.

Generating *t* Test Maps. To generate *t* test maps we first acquired four z-spectra of each sample using the same protocols as used in the other MRI experiments. Using an in-house MATLAB script based on prior publications.[17,28,29] We examined each voxel's intensity at 3.6 and −3.6 ppm from each experiment to generate the test populations. These were then compared using a one tailed unpaired *t* test. Voxels with a *p*-value worse than 0.05 were discarded, and the image was overlaid onto a spin echo image of the phantom.

Genetic Programming. POET algorithm is a multiplatform GP tool written in the Python programming language. The computational experiments were run on Michigan State University's High-Performance Computing Center (HPCC) systems. Each POET replicate uses only a single CPU core (2.5 GHz) and 8 gigabytes of RAM. At each generation of the experiment, 100 replicates of POET are executed in parallel using different random seeds to evolve protein-function models able to predict the CEST contrast of peptide sequences. These replicates allow POET to explore various regions of the search space at the same time to find fitter models. After the evolution of these models, the fittest one of them in each generation is employed for predicting new optimized peptides with respect to their CEST contrast levels. To do so, a population of 10,000 random peptide sequences is initialized and evolved by applying an iterative evolutionary algorithm. In this algorithm, each of the sequences in each iteration undergoes point mutation and is evaluated using the fittest previously evolved POET model. If a mutation is not beneficial then it is reverted, and the sequence will move to the next population unchanged. Otherwise, if the mutation is beneficial, the change is applied

https://doi.org/10.1021/acssynbio.2c00648
ACS Synth. Biol. 2023, 12, 1154−1163

to the sequence to be added to the next population. This process is performed for an arbitrary number of iterations (usually set to 1000) until fitter predicted peptide sequences are found. The top 10 predicted peptide sequences are chosen to be tested in the lab. Following lab measurements, these predicted peptides are added to the POET's training data set, increasing POET's chances to learn more meaningful motifs in the next generation of the experiment and enabling it to predict fitter and more optimized proteins in the future. At the very start, 42 data points (peptide sequences and their respective CEST contrast values) were available in the POET training data set. Furthermore, in each generation of the experiment, approximately 10 new predicted peptides were added to the data set after wet-lab measurements. In the final generation of the experiment, 128 data points were available causing each execution of POET to take up to 35 h to evolve fit sequence-function models. POET employs a novel GP representation specifically designed for motif discovery in protein engineering, which differs from previous GP representations utilized in the existing literature. Detailed explanations of the computational aspects of POET can be found in a sister article.[21]

CONCLUSIONS

Here we demonstrated that POET can be used to evolve peptides to produce substantially more CEST contrast than PLL after only a few generations. POET generated CESTides could potentially be assembled into the next generation of MRI reporter gene[62] with improved sensitivity over previous generations of reporters. Since POET requires only a small set of input peptide sequences and their corresponding quantitatively measured functions to evolve models that predict better peptide function, it is anticipated that POET can be used for the evolution of peptides in numerous applications.

ASSOCIATED CONTENT

Supporting Information

The Supporting Information is available free of charge at https://pubs.acs.org/doi/10.1021/acssynbio.2c00648.

> Figures relating to the properties of peptides developed using POET (Figure S1 and Figure S2), the amount of data that POET works with (Figure S3), and the SNR and CNR to accompany Figure 5 (Figure S4); An example POEM from POET to help a reader understand the nature of the models (Table S1) (PDF)

AUTHOR INFORMATION

Corresponding Authors

Wolfgang Banzhaf − *Department of Computer Science & Engineering, Michigan State University, East Lansing, Michigan 48823, United States*; Email: banzhafw@msu.edu

Assaf A. Gilad − *Department of Chemical Engineering and Materials Science, Michigan State University, East Lansing, Michigan 48823, United States; Department of Radiology, Michigan State University, East Lansing, Michigan 48823, United States*; orcid.org/0000-0002-7272-7570; Email: gilad@msu.edu

Authors

Alexander R. Bricco − *Department of Biomedical Engineering, Michigan State University, East Lansing, Michigan 48823, United States*; orcid.org/0000-0001-7960-6731

Iliya Miralavy − *Department of Computer Science & Engineering, Michigan State University, East Lansing, Michigan 48823, United States*

Shaowei Bo − *The Russell H. Morgan Department of Radiology and Radiological Sciences, Division of MR Research, Johns Hopkins University School of Medicine, Baltimore, Maryland 21218, United States*

Or Perlman − *Department of Biomedical Engineering and Sagol School of Neuroscience, Tel Aviv University, Tel Aviv 6997801, Israel; Athinoula A. Martinos Center for Biomedical Imaging, Department of Radiology, Massachusetts General Hospital and Harvard Medical School, Boston, Massachusetts 02138, United States*

David E. Korenchan − *Athinoula A. Martinos Center for Biomedical Imaging, Department of Radiology, Massachusetts General Hospital and Harvard Medical School, Boston, Massachusetts 02138, United States*; orcid.org/0000-0001-6152-5896

Christian T. Farrar − *Athinoula A. Martinos Center for Biomedical Imaging, Department of Radiology, Massachusetts General Hospital and Harvard Medical School, Boston, Massachusetts 02138, United States*

Michael T. McMahon − *The Russell H. Morgan Department of Radiology and Radiological Sciences, Division of MR Research, Johns Hopkins University School of Medicine, Baltimore, Maryland 21218, United States*

Complete contact information is available at: https://pubs.acs.org/10.1021/acssynbio.2c00648

Author Contributions

ARB, IL, WB, and AAG conceived the original idea of the research. ARB, IM, SB, OP, DEK, CTF, and MTM conducted research and analyzed the data. ARB, CTF, MTM, and AAG wrote the manuscript. ARB and AAG created figures. All authors took part in editing the manuscript and have given their approval for its publication.

Notes

The authors declare no competing financial interest.

ACKNOWLEDGMENTS

The authors acknowledge financial support from the NIH/NINDS: R01-NS098231; R01-NS104306 NIH/NIBIB: R01-EB031008; R01-EB030565; R01-EB031936; P41-EB024495 NIH/NIDDK: R01-DK121847, NIH S10-OD023406 and NSF 2027113. We thank Rita Martin for help in editing the manuscript and Dr. Jorden Schossau the helpful discussions.

REFERENCES

(1) Baker, D. What has de novo protein design taught us about protein folding and biophysics? *Protein Sci.* **2019**, *28* (4), 678−683.

(2) Romero, P. A.; Arnold, F. H. Exploring protein fitness landscapes by directed evolution. *Nat. Rev. Mol. Cell Biol.* **2009**, *10* (12), 866−76.

(3) Meyer, J. R.; Dobias, D. T.; Weitz, J. S.; Barrick, J. E.; Quick, R. T.; Lenski, R. E. Repeatability and Contingency in the Evolution of a Key Innovation in Phage Lambda. *Science* **2012**, *335* (6067), 428−432.

(4) Goldsmith, M.; Tawfik, D. S. Enzyme engineering: reaching the maximal catalytic efficiency peak. *Curr. Opin Struct Biol.* **2017**, *47*, 140−150.

(5) Koza, J. R. Genetic programming as a means for programming computers by natural selection. *Stat. Comput.* **1994**, *4* (2), 87−112.
(6) Banzhaf, W. x.; Francone, F. D.; Keller, R. E.; Nordin, P. *Genetic Programming: An Introduction: On the Automatic Evolution of Computer Programs and Its Applications*; Morgan Kaufmann Publishers Inc.: San Francisco, CA, 1998.
(7) Widera, P.; Garibaldi, J. M.; Krasnogor, N. GP challenge: evolving energy function for protein structure prediction. *Genetic Programming and Evolvable Machines* **2010**, *11* (1), 61−88.
(8) Vyas, R.; Bapat, S.; Goel, P.; Karthikeyan, M.; Tambe, S. S.; Kulkarni, B. D. Application of Genetic Programming (GP) Formalism for Building Disease Predictive Models from Protein-Protein Interactions (PPI) Data. *IEEE/ACM Trans. Comput. Biol. Bioinf.* **2018**, *15* (1), 27−37.
(9) Lehman, J.; Clune, J.; Misevic, D.; Adami, C.; Altenberg, L.; Beaulieu, J.; Bentley, P. J.; Bernard, S.; Beslon, G.; Bryson, D. M.; Chrabaszcz, P.; Cheney, N.; Cully, A.; Doncieux, S.; Dyer, F. C.; Ellefsen, K. O.; Feldt, R.; Fischer, S.; Forrest, S.; Frénoy, A.; Gagné, C.; Le Goff, L.; Grabowski, L. M.; Hodjat, B.; Hutter, F.; Keller, L.; Knibbe, C.; Krcah, P.; Lenski, R. E.; Lipson, H.; MacCurdy, R.; Maestre, C.; Miikkulainen, R.; Mitri, S.; Moriarty, D. E.; Mouret, J.-B.; Nguyen, A.; Ofria, C.; Parizeau, M.; Parsons, D.; Pennock, R. T.; Punch, W. F.; Ray, T. S.; Schoenauer, M.; Shulte, E.; Sims, K.; Stanley, K. O.; Taddei, F.; Tarapore, D.; Thibault, S.; Weimer, W.; Watson, R.; Yosinski, J. The Surprising Creativity of Digital Evolution: A Collection of Anecdotes from the Evolutionary Computation and Artificial Life Research Communities. *arXiv*, March 9, 2018, 1803.03453. DOI: 10.48550/arXiv.1803.03453.
(10) Koza, J. R. Human-competitive results produced by genetic programming. *Genet Program Evol M* **2010**, *11* (3−4), 251−284.
(11) van Zijl, P. C.; Yadav, N. N. Chemical exchange saturation transfer (CEST): what is in a name and what isn't? *Magn Reson Med.* **2011**, *65* (4), 927−48.
(12) Sherry, A. D.; Woods, M. Chemical Exchange Saturation Transfer Contrast Agents for Magnetic Resonance Imaging. *Annu. Rev. Biomed. Eng.* **2008**, *10*, 391−411.
(13) Goffeney, N.; Bulte, J. W.; Duyn, J.; Bryant, L. H., Jr.; van Zijl, P. C. Sensitive NMR detection of cationic-polymer-based gene delivery systems using saturation transfer via proton exchange. *J. Am. Chem. Soc.* **2001**, *123* (35), 8628−9.
(14) Liu, G.; Gilad, A. A.; Bulte, J. W.; van Zijl, P. C.; McMahon, M. T. High-throughput screening of chemical exchange saturation transfer MR contrast agents. *Contrast Media Mol. Imaging* **2010**, *5* (3), 162−70.
(15) McMahon, M. T.; Gilad, A. A.; DeLiso, M. A.; Berman, S. M.; Bulte, J. W.; van Zijl, P. C. New "multicolor" polypeptide diamagnetic chemical exchange saturation transfer (DIACEST) contrast agents for MRI. *Magn. Reson. Med.* **2008**, *60* (4), 803−812.
(16) Farrar, C. T.; Buhrman, J. S.; Liu, G.; Kleijn, A.; Lamfers, M. L.; McMahon, M. T.; Gilad, A. A.; Fulci, G. Establishing the Lysine-rich Protein CEST Reporter Gene as a CEST MR Imaging Detector for Oncolytic Virotherapy. *Radiology* **2015**, 140251.
(17) Gilad, A. A.; McMahon, M. T.; Walczak, P.; Winnard, P. T., Jr.; Raman, V.; van Laarhoven, H. W.; Skoglund, C. M.; Bulte, J. W.; van Zijl, P. C. Artificial reporter gene providing MRI contrast based on proton exchange. *Nat. Biotechnol.* **2007**, *25* (2), 217−219.
(18) Meier, S.; Gilad, A. A.; Brandon, J. A.; Qian, C. H.; Gao, E.; Abisambra, J. F.; Vandsburger, M. Non-invasive detection of adeno-associated viral gene transfer using a genetically encoded CEST-MRI reporter gene in the murine heart. *Sci. Rep.* **2018**, DOI: 10.1038/s41598-018-22993-4.
(19) Minn, I.; Bar-Shir, A.; Yarlagadda, K.; Bulte, J. W.; Fisher, P. B.; Wang, H.; Gilad, A. A.; Pomper, M. G. Tumor-specific expression and detection of a CEST reporter gene. *Magn Reson Med.* **2015**, *74* (2), 544−9.
(20) Perlman, O.; Ito, H.; Gilad, A. A.; McMahon, M. T.; Chiocca, E. A.; Nakashima, H.; Farrar, C. T. Redesigned reporter gene for improved proton exchange-based molecular MRI contrast. *Sci. Rep* **2020**, *10* (1), 20664.
(21) Miralavy, I.; Bricco, A. R.; Gilad, A. A.; Banzhaf, W. Using genetic programming to predict and optimize protein function. *PeerJ. Phys. Chem.* **2022**, *4*, e24.
(22) Bar-Shir, A.; Liang, Y.; Chan, K. W.; Gilad, A. A.; Bulte, J. W. Supercharged green fluorescent proteins as bimodal reporter genes for CEST MRI and optical imaging. *Chem. Commun. (Camb)* **2015**, *51* (23), 4869−71.
(23) Bar-Shir, A.; Liu, G.; Chan, K. W.; Oskolkov, N.; Song, X.; Yadav, N. N.; Walczak, P.; McMahon, M. T.; van Zijl, P. C.; Bulte, J. W.; Gilad, A. A. Human protamine-1 as an MRI reporter gene based on chemical exchange. *ACS Chem. Biol.* **2014**, *9* (1), 134−8.
(24) Yang, X.; Yadav, N. N.; Song, X.; Ray Banerjee, S.; Edelman, H.; Minn, I.; van Zijl, P. C.; Pomper, M. G.; McMahon, M. T. Tuning Phenols with Intra-Molecular Bond Shifted HYdrogens (IM-SHY) as diaCEST MRI Contrast Agents. *Chemistry* **2014**, *20*, 15824.
(25) Bar-Shir, A.; Bulte, J. W.; Gilad, A. A. Molecular Engineering of Nonmetallic Biosensors for CEST MRI. *ACS Chem. Biol.* **2015**, *10*, 1160.
(26) Bar-Shir, A.; Liu, G.; Liang, Y.; Yadav, N. N.; McMahon, M. T.; Walczak, P.; Nimmagadda, S. R.; Pomper, M. G.; Tallman, K. A.; Greenberg, M. M.; van Zijl, P. C.; Bulte, J. W.; Gilad, A. A. Transforming thymidine into a magnetic resonance imaging probe for monitoring gene expression. *J. Am. Chem. Soc.* **2013**, *135* (4), 1617−1624.
(27) McMahon, M. T.; Gilad, A. A.; Zhou, J.; Sun, P. Z.; Bulte, J. W.; van Zijl, P. C. Quantifying exchange rates in chemical exchange saturation transfer agents using the saturation time and saturation power dependencies of the magnetization transfer effect on the magnetic resonance imaging signal (QUEST and QUESP): Ph calibration for poly-L-lysine and a starburst dendrimer. *Magn Reson Med.* **2006**, *55* (4), 836−47.
(28) Gilad, A. A.; Israely, T.; Dafni, H.; Meir, G.; Cohen, B.; Neeman, M. Functional and molecular mapping of uncoupling between vascular permeability and loss of vascular maturation in ovarian carcinoma xenografts: The role of stroma cells in tumor angiogenesis. *Int. J. Cancer* **2005**, *117* (2), 202−11.
(29) Gilead, A.; Meir, G.; Neeman, M. The role of angiogenesis, vascular maturation, regression and stroma infiltration in dormancy and growth of implanted MLS ovarian carcinoma spheroids. *Int. J. Cancer* **2004**, *108* (4), 524−31.
(30) Grantham, R. Amino Acid Difference Formula to Help Explain Protein Evolution. *Science* **1974**, *185*, 862−864.
(31) Li, A. X.; Wojciechowski, F.; Suchy, M.; Jones, C. K.; Hudson, R. H.; Menon, R. S.; Bartha, R. A sensitive PARACEST contrast agent for temperature MRI: Eu3+-DOTAM-glycine (Gly)-phenylalanine (Phe). *Magn Reson Med.* **2008**, *59* (2), 374−81.
(32) Wu, Y.; Soesbe, T. C.; Kiefer, G. E.; Zhao, P.; Sherry, A. D. A responsive europium(III) chelate that provides a direct readout of pH by MRI. *J. Am. Chem. Soc.* **2010**, *132* (40), 14002−3.
(33) Chan, K. W.; Liu, G.; Song, X.; Kim, H.; Yu, T.; Arifin, D. R.; Gilad, A. A.; Hanes, J.; Walczak, P.; van Zijl, P. C.; Bulte, J. W.; McMahon, M. T. MRI-detectable pH nanosensors incorporated into hydrogels for *in vivo* sensing of transplanted-cell viability. *Nat. Mater.* **2013**, *12* (3), 268−75.
(34) Yoo, B.; Pagel, M. D. A PARACEST MRI contrast agent to detect enzyme activity. *J. Am. Chem. Soc.* **2006**, *128* (43), 14032−3.
(35) Liu, G.; Moake, M.; Har-el, Y.-e.; Long, C. M.; Chan, K. W. Y.; Cardona, A.; Jamil, M.; Walczak, P.; Gilad, A. A.; Sgouros, G.; van Zijl, P. C. M.; Bulte, J. W. M.; McMahon, M. T. In vivo multicolor molecular MR imaging using diamagnetic chemical exchange saturation transfer liposomes. *Magn. Reson. Med.* **2012**, *67*, 1106.
(36) Trokowski, R.; Ren, J.; Kalman, F. K.; Sherry, A. D. Selective sensing of zinc ions with a PARACEST contrast agent. *Angew. Chem., Int. Ed. Engl.* **2005**, *44* (42), 6920−3.
(37) Haris, M.; Cai, K.; Singh, A.; Hariharan, H.; Reddy, R. In vivo mapping of brain myo-inositol. *Neuroimage* **2011**, *54* (3), 2079−85.
(38) van Zijl, P. C.; Jones, C. K.; Ren, J.; Malloy, C. R.; Sherry, A. D. MRI detection of glycogen *in vivo* by using chemical exchange

saturation transfer imaging (glycoCEST). *Proc. Natl. Acad. Sci. U. S. A.* **2007**, *104* (11), 4359−64.
(39) Walker-Samuel, S.; Ramasawmy, R.; Torrealdea, F.; Rega, M.; Rajkumar, V.; Johnson, S. P.; Richardson, S.; Goncalves, M.; Parkes, H. G.; Arstad, E.; Thomas, D. L.; Pedley, R. B.; Lythgoe, M. F.; Golay, X. In vivo imaging of glucose uptake and metabolism in tumors. *Nat. Med.* **2013**, *19* (8), 1067−72.
(40) Song, X.; Airan, R. D.; Arifin, D. R.; Bar-Shir, A.; Kadayakkara, D. K.; Liu, G.; Gilad, A. A.; van Zijl, P. C.; McMahon, M. T.; Bulte, J. W. Label-free *in vivo* molecular imaging of underglycosylated mucin-1 expression in tumour cells. *Nat. Commun.* **2015**, *6*, 6719.
(41) Ling, W.; Regatte, R. R.; Navon, G.; Jerschow, A. Assessment of glycosaminoglycan concentration *in vivo* by chemical exchange-dependent saturation transfer (gagCEST). *Proc. Natl. Acad. Sci. U. S. A.* **2008**, *105* (7), 2266−70.
(42) Vandsburger, M.; Vandoorne, K.; Oren, R.; Leftin, A.; Mpofu, S.; Delli Castelli, D.; Aime, S.; Neeman, M. Cardio-chemical exchange saturation transfer magnetic resonance imaging reveals molecular signatures of endogenous fibrosis and exogenous contrast media. *Circ. Cardiovasc. Imaging* **2015**, DOI: 10.1161/CIRCIMAGING.114.002180.
(43) Haris, M.; Singh, A.; Cai, K.; Kogan, F.; McGarvey, J.; Debrosse, C.; Zsido, G. A.; Witschey, W. R.; Koomalsingh, K.; Pilla, J. J.; Chirinos, J. A.; Ferrari, V. A.; Gorman, J. H.; Hariharan, H.; Gorman, R. C.; Reddy, R. A technique for *in vivo* mapping of myocardial creatine kinase metabolism. *Nat. Med.* **2014**, *20* (2), 209−14.
(44) Choi, J.; Kim, K.; Kim, T.; Liu, G.; Bar-Shir, A.; Hyeon, T.; McMahon, M. T.; Bulte, J. W. M.; Fisher, J. P.; Gilad, A. A. Multimodal imaging of sustained drug release from 3-D poly-(propylene fumarate) (PPF) scaffolds. *J. Controlled Release* **2011**, *156* (2), 239−245.
(45) Airan, R. D.; Bar-Shir, A.; Liu, G.; Pelled, G.; McMahon, M. T.; van Zijl, P. C.; Bulte, J. W.; Gilad, A. A. MRI biosensor for protein kinase A encoded by a single synthetic gene. *Magn Reson Med.* **2012**, *68* (6), 1919−23.
(46) Liu, G.; Liang, Y.; Bar-Shir, A.; Chan, K. W.; Galpoththawela, C. S.; Bernard, S. M.; Tse, T.; Yadav, N. N.; Walczak, P.; McMahon, M. T.; Bulte, J. W.; van Zijl, P. C.; Gilad, A. A. Monitoring enzyme activity using a diamagnetic chemical exchange saturation transfer magnetic resonance imaging contrast agent. *J. Am. Chem. Soc.* **2011**, *133* (41), 16326−9.
(47) Alon, L.; Kraitchman, D. L.; Schar, M.; Cortez, A.; Yadav, N. N.; Krimins, R.; Johnston, P. V.; McMahon, M. T.; van Zijl, P. C. M.; Nimmagadda, S.; Pomper, M. G.; Bulte, J. W. M.; Gilad, A. A. Molecular imaging of CXCL12 promoter-driven HSV1-TK reporter gene expression. *Biotechnol. Bioprocess Eng.* **2018**, *23* (2), 208−217.
(48) Gilad, A. A.; Winnard, P. T., Jr.; van Zijl, P. C.; Bulte, J. W. Developing MR reporter genes: promises and pitfalls. *NMR Biomed* **2007**, *20* (3), 275−90.
(49) Bar-Shir, A.; Liu, G.; Song, X.; Walczak, P.; McMahon, M. T.; van Zijl, P. C.; Bulte, J. W.; Gilad, A. A. Genetic Engineering of Human Protamine-1 for use as MRI Reporter Gene Based on Proton Exchange. In *Proceedings of the 19th Scientific Meeting*, International Society for Magnetic Resonance in Medicine, Montreal, Canada, 2011; p 1725.
(50) Isaksson, K.; Akerberg, D.; Posaric-Bauden, M.; Andersson, R.; Tingstedt, B. In vivo toxicity and biodistribution of intraperitoneal and intravenous poly-L-lysine and poly-L-lysine/poly-L-glutamate in rats. *J. Mater. Sci. Mater. Med.* **2014**, *25* (5), 1293−9.
(51) Ayyappan, J. P.; Sami, H.; Rajalekshmi, D. C.; Sivakumar, S.; Abraham, A. Immunocompatibility and toxicity studies of poly-L-lysine nanocapsules in sprague-dawley rats for drug-delivery applications. *Chem. Biol. Drug Des* **2014**, *84* (3), 292−9.
(52) Kanada, M.; Linenfelser, L.; Cox, E.; Gilad, A. A. A Dual-Reporter Platform for Screening Tumor-Targeted Extracellular Vesicles. *Pharmaceutics* **2022**, *14* (3), 475.
(53) Lee, H. D.; Grady, C. J.; Krell, K.; Strebeck, C.; Good, N. M.; Martinez-Gomez, N. C.; Gilad, A. A. A Novel Protein for the Bioremediation of Gadolinium Waste. *bioRxiv*, February 28, 2023, 2023.01.05.522788. DOI: 10.1101/2023.01.05.522788.
(54) Ricker, B.; Mitra, S.; Castellanos, E. A.; Grady, C. J.; Pelled, G.; Gilad, A. A. Proposed three-phenylalanine motif involved in magnetoreception signaling of an Actinopterygii protein expressed in mammalian cells. *bioRxiv*, December 9, 2022, 2022.12.08.519643. DOI: 10.1101/2022.12.08.519643.
(55) Grady, C. J.; Schossau, J.; Ashbaugh, R. C.; Pelled, G.; Gilad, A. A. A putative design for electromagnetic activation of split proteins for molecular and cellular manipulation. *bioRxiv*, November 30, 2022, 2022.11.30.518522. DOI: 10.1101/2022.11.30.518522.
(56) Petersen, E. D.; Lapan, A. P.; Fillion, A. J.; Crespo, E. L.; Lambert, G. G.; Zanca, A. T.; Orcutt, R.; Hochgeschwender, U.; Shaner, N. C.; Gilad, A. A. Bioluminescent Genetically Encoded Glutamate Indicator for Molecular Imaging of Neuronal Activity. *bioRxiv*, January 14, 2022, 2021.06.16.448690. DOI: 10.1101/2021.06.16.448690.
(57) Kim, M.; Gillen, J.; Landman, B. A.; Zhou, J.; van Zijl, P. C. Water saturation shift referencing (WASSR) for chemical exchange saturation transfer (CEST) experiments. *Magn Reson Med.* **2009**, *61* (6), 1441−50.
(58) Liu, G.; Song, X.; Chan, K. W.; McMahon, M. T. Nuts and bolts of chemical exchange saturation transfer MRI. *NMR in biomedicine* **2013**, *26* (7), 810−28.
(59) Xu, X.; Lee, J. S.; Jerschow, A. Ultrafast scanning of exchangeable sites by NMR spectroscopy. *Angew. Chem., Int. Ed. Engl.* **2013**, *52* (32), 8281−4.
(60) Zaiß, M.; Schmitt, B.; Bachert, P. Quantitative separation of CEST effect from magnetization transfer and spillover effects by Lorentzian-line-fit analysis of z-spectra. *J. Magn. Reson.* **2011**, *211* (2), 149−155.
(61) Cohen, O.; Huang, S.; McMahon, M. T.; Rosen, M. S.; Farrar, C. T. Rapid and quantitative chemical exchange saturation transfer (CEST) imaging with magnetic resonance fingerprinting (MRF). *Magn. Reson. Med.* **2018**, *80* (6), 2449−2463.
(62) Gilad, A. A.; Bar-Shir, A.; Bricco, A. R.; Mohanta, Z.; McMahon, M. T. Protein and peptide engineering for chemical exchange saturation transfer imaging in the age of synthetic biology. *NMR Biomed* **2022**, e4712.